



Spectroscopic Characterization of the Electronic Structure, Chemical Bonding, and Band Gap in Thermally Annealed Polycrystalline Ga_2O_3 Thin Films

Nanthakishore Makeswaran,¹ Anil K. Battu,¹ Roy Swadipta,¹ Felicia S. Manciu,² and C. V. Ramana^{1,2}

¹Center for Advanced Materials Research (CMR), University of Texas at El Paso, El Paso, Texas 79968, USA

²Department of Physics, University of Texas at El Paso, El Paso, Texas 79968, USA

Gallium oxide (Ga_2O_3) thin films were deposited onto Si(100) substrates at 500°C by sputtering the Ga_2O_3 ceramic target. The effect of thermal annealing in the temperature range of 500–900°C on the crystal structure, chemical bonding, electronic structure, and bandgap of polycrystalline Ga_2O_3 films was evaluated. Thermal annealing induced improvement in the structural quality and packing density of the Ga_2O_3 films as evident from X-ray diffraction and Raman spectroscopic analyses. X-ray photoelectron spectroscopic (XPS) analyses indicate the binding energies (BE) of the Ga 2p doublet i.e., the $\text{Ga 2p}_{3/2}$ and $\text{Ga 2p}_{1/2}$ peaks, are located at 1118.0 and 1145.0 eV, respectively, characterizing gallium in its highest chemical oxidation state (Ga^{3+}) in the as-deposited films. The core level XPS spectra of O 1s indicate that the peak is centered at a BE~531 eV, which is also characteristic of Ga-O bonds in the Ga_2O_3 phase. No significant changes were seen in the electronic structure, especially in terms of chemical valence of Ga ions and Ga-O bonds, as function of thermal annealing in the entire temperature range of 500–900°C. However, the presence of carbonyl functional groups become evident in XPS for samples under thermal annealing. Raman analysis also reveals an obvious blueshift for the high-frequency stretching and bending of the GaO_4 tetrahedra, which structurally form the $\beta\text{-}\text{Ga}_2\text{O}_3$, with confinement. The bandgap determined from spectrophotometry measurements varies in the range of 4.94–4.78 eV for a variation in annealing temperature in the range of 500–900°C. A correlation between annealing temperature, electronic structure, chemical bonding and bandgap in Ga_2O_3 films is established.

© The Author(s) 2019. Published by ECS. This is an open access article distributed under the terms of the Creative Commons Attribution 4.0 License (CC BY, <http://creativecommons.org/licenses/by/4.0/>), which permits unrestricted reuse of the work in any medium, provided the original work is properly cited. [DOI: 10.1149/2.0461907jss]



Manuscript submitted March 22, 2019; revised manuscript received June 17, 2019. Published July 11, 2019. *This paper is part of the JSS Focus Issue on Gallium Oxide Based Materials and Devices.*

Wide bandgap oxides have been the subject of intense research in recent years in view of their wide range of technological applications in electronics, photonics, catalysis, electro-optics, integrated sensors, magneto-electronics, and photovoltaics.^{1–9} Very high level of tolerance to the high applied electric fields and high break-down electric field are quite attractive features of these oxides for utilization in high power and high frequency devices.^{5–9} Gallium oxide (Ga_2O_3), one among these wide bandgap oxides, is potentially applicable in a broad range of aforementioned technological applications. Ga_2O_3 is the second largest wide bandgap material with a bandgap of ~4.9 eV.¹⁰ Ga_2O_3 exhibits diverse structures, quite interesting material properties, and chemical and thermodynamic stability.^{6,7} Thin films and nanostructures of Ga_2O_3 find numerous applications in high-temperature sensors, electronics, luminescent phosphors, antireflection coatings, lithium batteries and solar cells.^{11–15} Gallium oxide exhibits polymorphism; the α , β , γ , δ , and ϵ phases of Ga_2O_3 are widely known.^{15–19} Among these polymorphs, monoclinic $\beta\text{-}\text{Ga}_2\text{O}_3$ is thermally stable with a predicted high breakdown field 8 MV/cm.^{6,20} $\beta\text{-}\text{Ga}_2\text{O}_3$ exhibits n-type conductivity, which is related to donor centers involving oxygen vacancies and/or impurities.^{6,16,17} The high thermal stability of $\beta\text{-}\text{Ga}_2\text{O}_3$ is quite useful in the design and development of high-temperature chemical sensors, which can be readily used in automotive industry and power plants.^{14,15} Furthermore, the high-temperature stability coupled with deep ultraviolet transparency makes Ga_2O_3 based materials as the potential candidates for chemical sensors in extreme environments and transparent electrodes in UV optoelectronics, photonics, and thin-film transistors. However, in all these applications, fundamental understanding of the structure and properties is the key to achieving enhanced device performance. In this work, nanocrystalline Ga_2O_3 films were produced using sputter-deposition. The effect of post-deposition annealing on the structure and chemistry of the Ga_2O_3 films was evaluated by the combined use of X-ray photoelectron and Raman spectroscopic measurements.

Experimental

Deposition of Ga_2O_3 films.—Nanocrystalline Ga_2O_3 films were fabricated on silicon (Si) (100) wafers by RF-sputtering. All the substrates were cleaned and dried with nitrogen before placing them into the vacuum chamber, which is evacuated to a base pressure of $\sim 10^{-6}$ Torr. The deposition was employed by sputtering of Ga_2O_3 ceramic target. The Ga_2O_3 ceramic target (Plasmaterials, Inc.) of 2 in. diameter and 99.999% purity. The Ga_2O_3 target was mounted on a 2 in. sputter gun, which were placed at a distance of 7 cm from the substrate. Initially a sputtering power of 40 W was applied to target while introducing high-purity argon (Ar) gas into the chamber to ignite the plasma. Once the plasma was ignited the power for the target was gradually increased to their respective sputtering power for the deposition. The flow of Ar and oxygen (O_2) were controlled using an MKS mass flow meters. Before each deposition, the target was pre-sputtered for 15–20 min with a closed shutter above the gun. The deposition time kept constant which is 3 hours for the sputtering power of 100 W to produce Ga-oxide films with a thickness of ~200 nm. The samples were deposited at substrate temperatures (T_s) 500°C, which is optimum for producing nanocrystalline β -phase Ga_2O_3 films. Substrate rotation is maintained during the entire deposition time to ensure uniform coverage on the substrate surface. The sample was then annealed between 600 to 900°C for 1 h in air.

Characterization of Ga_2O_3 films.—X-ray diffraction (XRD) measurements on Ga_2O_3 films deposited on Si were performed using a Bruker D8 Advance X-ray diffractometer. All the measurements were made ex-situ as a function of annealing temperature. XRD patterns were recorded using $\text{Cu K}\alpha$ radiation ($\lambda = 1.54056 \text{ \AA}$) at room temperature. The chemical analysis of the as deposited and annealed Ga_2O_3 thin films was made employing X-ray photoelectron spectroscopy (XPS). The samples were mounted on a Cu stub with the help of double-sided Cu tape, and analyzed using a calibrated Kratos Axis Ultra DLD spectrometer (Kratos Analytical, Manchester UK) which has a high performance $\text{Al K}\alpha$ (1486.7 eV) spherical mirror

¹E-mail: rvchintalapalle@utep.edu

analyzer. A piece of Cu tape was attached on the sample surface up to the stub surface in order to avoid charging issues (e.g. peak broadening, peak shifting etc.). In spite of this, the charge neutralizer was used to compensate the surface charging effects. Survey and multiple high-resolution scans were collected at a pass energy of 160 and 40 eV respectively. Survey spectra were obtained over the binding energy (BE) range of 1400–(-5) eV with a step size of 0.5 eV whereas, high resolution scans were obtained with an energy step of 0.1 eV. The analysis area which is basically $700 \times 300 \mu\text{m}$ area is referred to the full width at half maximum (fwhm) of 0.70 eV for Ag 3d5/2 collected at 40 eV pass energy. High resolution scans were obtained for Ga 2p, Ga 3d, O 1s, and C 1s peaks. Each high-resolution scan was recorded for at least 8 sweeps in order to get well resolved spectra. Both survey and high-resolution scans were collected under ultra-high vacuum (UHV- 2×10^{-9} torr) condition. C 1s binding energy at 284.8 eV was used for the charge reference. Survey and high-resolution spectra were analyzed using CasaXPS V2.3.16 to obtain the atomic composition and for more in-depth studies respectively. Peak areas were calculated employing both Gaussian/Lorentzian (GL(30)) line shape and line asymmetry and Shirley background subtraction whereas, compositional analysis were performed using the relative sensitivity factors for the instrument. At least three spots were chosen per each sample in order to maintain good statistical index.

The Raman measurements were acquired at room temperature with an *alpha 300R WITec* confocal Raman system (WITec Inc., Ulm, Germany). The 532 nm excitation of a frequency-doubled neodymium-doped yttrium-aluminum-garnet (Nd:YAG) laser that was kept at a low power output of a few mW, and a 20X objective lens with a numerical aperture of 0.4 were used for data acquisition. The Raman signal was detected by a 1024×127 pixel peltier cooled CCD camera with a spectral resolution of 4 wavenumbers. Accumulation of 20 Raman spectra, each spectrum recorded for 500 milliseconds, with an overall Raman acquisition time of 10 seconds per sample was employed. A normalization to the Si vibrational frequency was performed for the samples grown on Si substrates. Also, appropriate background subtractions were performed for all Raman spectra. The bandgap of as deposited and annealed Ga_2O_3 thin films was determined using spectrophotometry measurements and analysis. Spectral characteristics of as deposited and annealed Ga_2O_3 thin films were measured employing a Cary 5000 UV–vis-NIR double-beam spectrophotometer. Samples deposited on quartz were used for spectrophotometry measurements.

Results and Discussion

The GIXRD spectra of as-deposited and annealed Ga_2O_3 thin films are shown in Fig. 1. It is evident from the patterns that the annealing temperature significantly affect the crystal structure. The GIXRD pattern of nc- Ga_2O_3 corresponds to the monoclinic β -phase having space group of C2/m with peaks (-201), (400), (002), and (-204) corresponds to 2θ values of 18.95, 30.05, 31.74, and 64.17 respectively according to JCPDS (00-043-1012) for the film deposited at 500°C. The film annealed at 600°C, the crystallinity did not change much. Whereas, at the annealing temperature of 700°C, the peak intensity is increased and at the same time (104), (113) and (-211) peaks started appearing. This is an indication that the film crystal quality and texturing evolves with thermal annealing. Further increasing the annealing temperatures to 900°C, the XRD spectra were clearly enhanced grown preferentially in (400) and (-201) orientations. Especially the (400) peak intensity was increased and at the same time peak became sharper indicating a higher degree of crystallization. The GIXRD spectra clearly indicate the polycrystalline nature of the Ga_2O_3 thin films, the peaks are majorly intensified.

The surface chemistry of as-deposited and annealed Ga_2O_3 thin films was analyzed using X-ray photoelectron spectroscopy (XPS). Figure 2 represents the survey spectra of the Ga-oxide thin films. The C 1s signal evident in all survey spectra is owing to the adventitious carbon adsorbed on the film surface due to exposure in air while transferring the sample from the growth chamber to the XPS load lock. Though it is possible to remove it completely from the sample

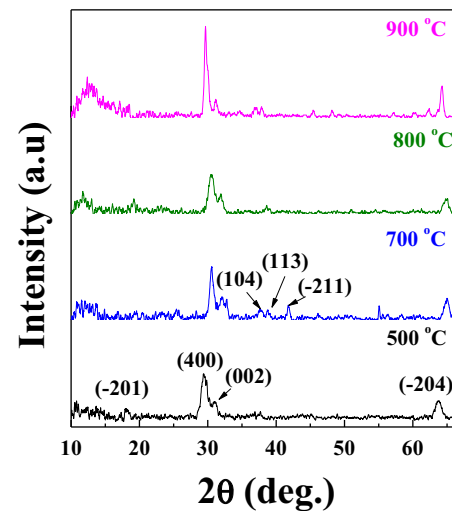


Figure 1. XRD patterns of as-deposited and annealed Ga_2O_3 films. Evident from the XRD patterns, all the Ga_2O_3 films crystallize in β -phase; however, the annealing temperature strongly influences the peak evolution and, hence, the structure of Ga_2O_3 films.

surface by sputtering with the inert gas (e.g. Ar) but it may significantly affect the surface chemistry. Also, it should be noted that the XPS analyses were made on the as-deposited and annealed films, where the surface roughness effects may present. For clarity and understanding purposes, the root-mean-square surface roughness value noted for as-deposited Ga_2O_3 films was ~ 1 nm, which then increases with annealing temperature. The Ga_2O_3 films annealed at 700°C exhibit the highest roughness (~ 5 nm) values while the roughness decreases to < 2 nm for annealing temperatures 800–900°C.

The core level photoelectron spectra of the Ga 2p doublet shown in Fig. 3. The BE values for the Ga 2p_{3/2} and Ga 2p_{1/2} peaks are

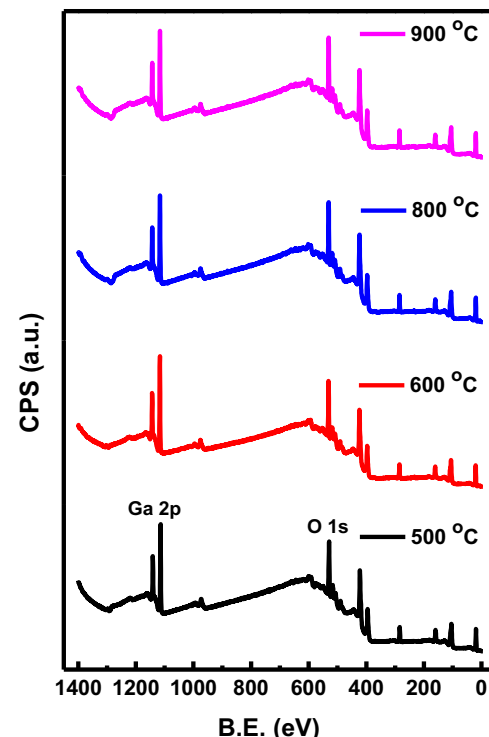


Figure 2. XPS survey spectra of as-deposited and annealed Ga_2O_3 films.

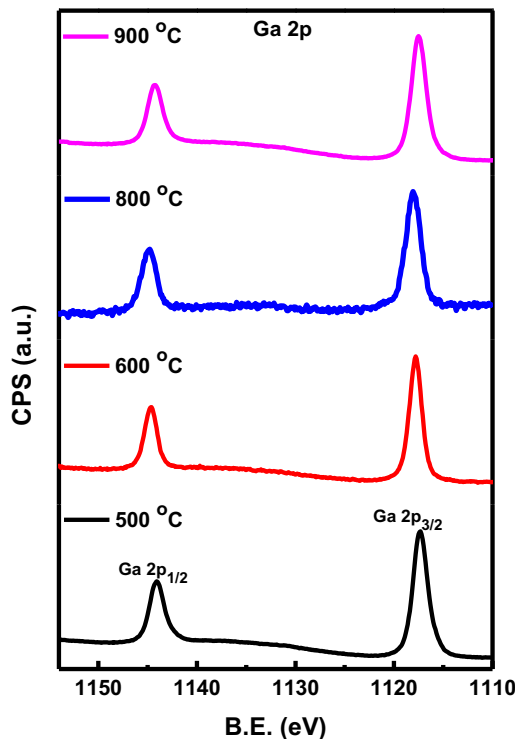


Figure 3. The Ga 2p core level XPS data of as-deposited and annealed Ga-oxide films. While the Ga 2p peak positions and data confirm the existence of Ga in its highest oxidation state in the films, the effect of annealing is insignificant for the BE of Ga 2p_{3/2} and Ga 2p_{1/2} peaks of the doublet.

1117.5 and 1144.2 eV, respectively. Though, Ga 3d high resolution peaks were also collected, but the Ga 2p region was chosen over the Ga 3d region for analysis in order to avoid the interference of the Ga 3d peak with the O 2s peak.^{7,10} The chemical shifts observed for both the Ga 2p and Ga 3d peaks are quite similar. Probing the Ga 2p region provides information about the nature of the Ga-O chemical bonding and Ga valence state in the as-deposited and annealed films. These values are almost consistent and do not exhibit any large shift. No variation in full-width at half-maximum (FWHM) was observed for these peaks. The BE of Ga 2p doublet peaks (i.e. Ga 2p_{3/2} and Ga 2p_{1/2}) for metallic Ga are: 1117.0 and 1144.0 eV respectively. The as-deposited Ga-oxide thin films show a positive shift in the BE in comparison to the metallic gallium. Shift in BE occurs mainly due to the redistribution of the electronic cloud around the constituent atoms.^{7,8,16,21} Therefore, these shifts in Ga 2p BE can facilitate to extract information about the exact oxidation state(s) of Ga in the as grown films. Based on these considerations and comparing with the available literature values, it can be concluded that the Ga exists in the highest valence state (i.e. Ga³⁺) within the films deposited on the Si substrate.^{7,8,16}

The core level XPS data of the O 1s peak also revealed fascinating information about the surface chemistry of the as-deposited and annealed Ga-oxide films. The high resolution XPS spectra for O 1s peak are shown in Fig. 4. The O 1s peak is not symmetric at all in the samples. As shown in Fig. 4, the O 1s peak for the samples can be resolved mostly into three components. The main peak is centered around BE 530.7 eV. As the annealing temperature increases, the main peak shifts toward higher BE side. This can be correlated with the increasing amount of crystallinity with increasing annealing temperature though XPS solely cannot confirm the fact. Two small shoulders to the left side of the main peak can be observed at BE 531.9 and 532.9 eV for the 800 and 900°C annealed samples respectively. Though, the 531.9 eV BE peak is omnipresent in all the samples, but 500°C sample shows a shoulder to the right of the main peak at around BE 529 eV which is

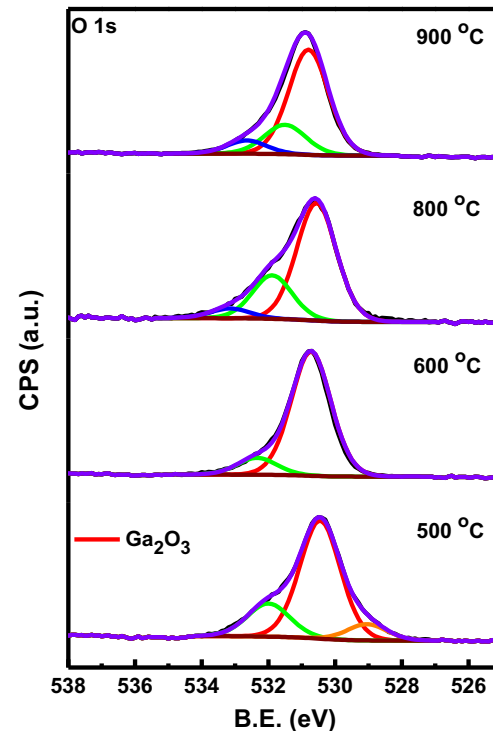


Figure 4. The O 1s core level XPS data of as-deposited and annealed Ga-oxide films.

not evident in other samples. It has been reported in the literature that the O 1s peak for the pure Ga-oxide thin films occurs generally at a BE of 530.8 eV, which is a salient characteristic feature of the Ga-O bonding with the highest oxidation state of Ga (i.e. Ga³⁺).^{7,16,21} Comparing the 532.9 eV BE with the available literature, it seems that the 800 and 900°C samples show sign of underneath oxidized substrate (i.e. SiO₂) surface. From this observation, two possibilities can be anticipated which are as follows: the coverage of the Ga₂O₃ thin film is not uniform throughout the substrate surface and/or the thin film thickness is more or less 7 nm which falls within the efficient probing depth of a XPS which is a highly surface sensitive characterization. For 500°C sample, the peak located at BE 529 is a satellite peak of O 1s which generally appears at lower BE's. The less intense peak at BE 531.9 eV which is present in all the samples, can be easily attributed to the adventitious carbon bonded with the O₂. The adventitious carbon might have adsorbed onto the film surface during sample transfer to the XPS system from the fabrication chamber.⁷

The micro-Raman spectra of the thin films of β -Ga₂O₃ (as-deposited at a Si substrate temperature of 500°C and further annealed at different temperatures) are presented in Fig. 5a. For a better understanding and assignment of the observed vibrational modes, as well as for an easier comparison with those already reported in the literature for bulk β -Ga₂O₃,^{22,23} we also present in Fig. 5b the Raman spectrum of a bulk sample. Figure 5a reveals no change in the positions of the Raman peaks at 618, 673, and 821 cm⁻¹ with increasing annealing temperature. However, closer inspection reveals slight increases in the intensities of these Raman features, especially for that at 618 cm⁻¹. This intensity increase is an indicator of higher sample crystallinity at a higher annealing temperature, as previously observed from samples' XRD patterns.

Comparison between the Raman spectra presented in Figs. 5a and 5b reveals an obvious blueshift for the high-frequency stretching and bending of the GaO₄ tetrahedra, which structurally form the β -Ga₂O₃, with confinement. For example, the Raman peak at 652 cm⁻¹ shifts to 673 cm⁻¹, and the Raman line at 765 cm⁻¹ shifts to 821 cm⁻¹. A redshift is seen for the 628 cm⁻¹ vibrational line of the bulk

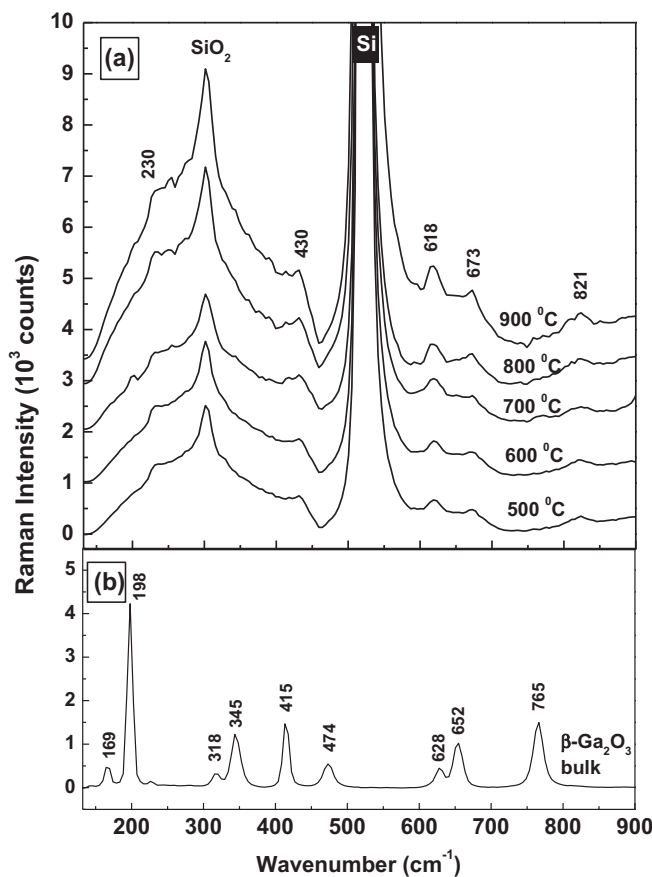


Figure 5. (a) Raman spectra of thin films of β - Ga_2O_3 , as-deposited at a Si substrate temperature of 500°C and further annealed at 600°C, 700°C, 800°C, and 900°C. The spectra are vertically translated for easier visualization, and appropriately labeled. (b) Raman spectrum of bulk β - Ga_2O_3 powder sample.

sample to a 618 cm^{-1} location in the thin films. Similar behavior, with quite large frequency shifts of about $15 \pm 5\text{ cm}^{-1}$, was previously reported for low-dimensional β - Ga_2O_3 nanowires, and associated with the presence of impurities and point defects, twins, and crystallite aggregation, besides that originating from the expected phononic effects of size-confinement.²² Unfortunately, in the low- and mid-frequency regions, which correspond to the libration/translational modes and deformations of Ga_2O_6 octahedra modes,^{22,23} respectively, dominant interference from the Si substrate signature at 521 cm^{-1} and from the broad SiO_2 feature centered around 303 cm^{-1} is seen in the Raman spectra presented in Fig. 5a. Thus, although the weak shoulder at 230 cm^{-1} and the weak band at 430 cm^{-1} could be associated with the bulk frequencies blueshifted from 198 cm^{-1} and 415 cm^{-1} , respectively, they could also be attributed to the oxidized Si layer underneath the thin film sample deposit. The increase in the intensity of the Raman band at 303 cm^{-1} observed for annealing temperatures of 800°C and 900°C suggests an increase in the thickness of this unwanted oxidized Si layer, corroborating previous XPS findings.

The purpose of spectrophotometry measurements was primarily to evaluate the optical transparency and to determine the bandgap in as-deposited and annealed Ga_2O_3 films. Figure 6 shows the spectral transmission characteristics of as-deposited and annealed Ga_2O_3 thin films. There was no absorption in the visible range which is 400–700 nm and all the films exhibit a sharp absorption edge existed at around 245 nm. In general, absorption edge with in the UV region are due to the electronic transitions from valance band to conduction band. Whereas, the cutoff wavelength is determined by the bandgap energy. For β - Ga_2O_3 films with a direct bandgap,²⁴ the absorption follows a

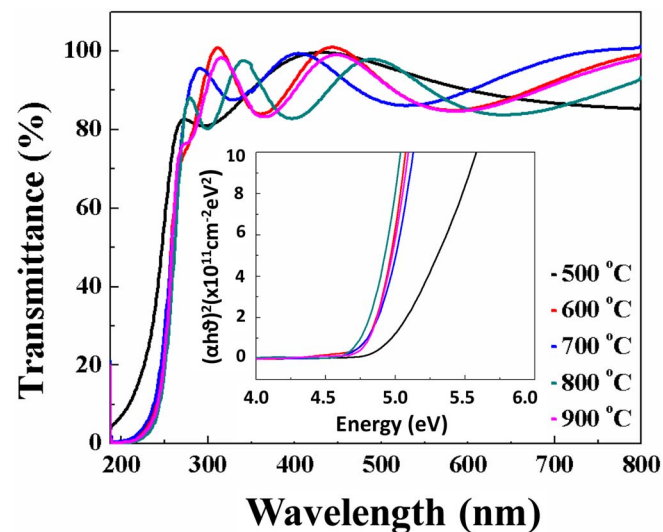


Figure 6. Spectral transmittance characteristics of Ga_2O_3 thin films annealed at different temperatures. Inset shows the absorption data calculated and analyzed to determine the bandgap of Ga_2O_3 thin films.

power law of the form

$$(\alpha h\nu) = B(h\nu - E_g)^{1/2} \quad [1]$$

where $h\nu$ is the energy of the incident photon, α - the absorption coefficient, B - the absorption edge width parameter, E_g the bandgap. The optical absorption coefficient, α , is evaluated using the standard relation taking the thickness into account.²¹ The absorption data and the plots obtained for the as deposited and annealed Ga_2O_3 films are shown in the inset of Figure 6. The bandgap is determined by fitting the linear region of the plot $(\alpha h\nu)^2$ vs $h\nu$. It is evident from the data (Fig. 6, inset) that $(\alpha h\nu)^2$ vs $h\nu$ results in linear plots within the high absorption region suggesting that direct allowed transitions across E_g of Ga_2O_3 thin films. Regression analysis and extrapolating the linear region of the plot to $h\nu = 0$ provide the bandgap value.

The E_g variation as a function of temperature for as deposited and annealed films Ga_2O_3 is presented in Figure 7. The bandgap values of the as-deposited films was 4.94 eV. The bandgap value decreases with increasing annealing temperature. The E_g of annealed Ga_2O_3 varies in the range of 4.94–4.78 eV. The lowest, minimum value of 4.74 eV was attained for annealing at 800°C and then then it slightly increases to 4.78 eV at 900°C. The lower E_g values of annealed Ga_2O_3 films at 800–900°C may be due to the improved crystallinity of the samples as

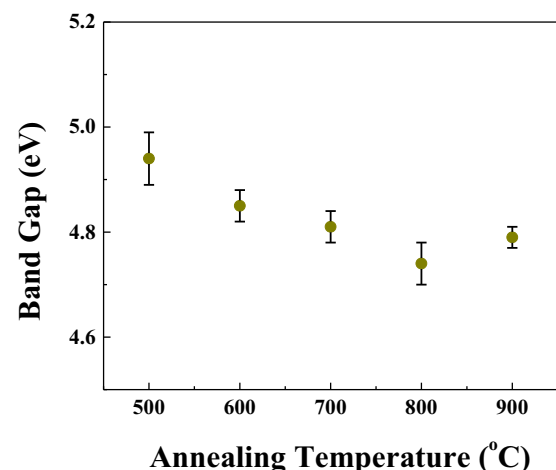


Figure 7. Bandgap variation of Ga_2O_3 thin films with annealing temperature.

evidenced from XRD studies. These results in good agreement with those reported for Ga_2O_3 films deposited by metal-organic chemical vapor deposition (MOCVD)²⁵ and laser-based molecular beam epitaxy (MBE).²⁶ Ga_2O_3 films deposited by MOCVD exhibited an amorphous-to-crystalline structural transformation with a better crystalline quality and smoother surface when annealed at 900°C.²⁵ Because of the better crystalline quality, the 900°C annealed MOCVD Ga_2O_3 films also attained the minimum optical bandgap coupled with a very high transparency.²⁵ The optical transmittance spectra of $\beta\text{-}\text{Ga}_2\text{O}_3$ shows fluctuations of transmittance curves caused by the interference of reflections from the surfaces and interfaces of the sample. While similar Eg values were obtained upon annealing, the 900°C annealed MOCVD films attained the minimum optical bandgap, because at that annealed temperature is when films have the best crystallinity.²⁵ Zhaoqing Feng et al deposited $\beta\text{-}\text{Ga}_2\text{O}_3$ thin films using laser-assisted molecular beam epitaxy (MBE) at 600°C.²⁶ The MBE $\beta\text{-}\text{Ga}_2\text{O}_3$ epilayers annealed at different temperatures for different durations in air and oxygen indicated the evolution in their optical behavior.²⁶ Annealing at 800–900°C for 30 or 60 minutes make the samples close to β -phase Ga_2O_3 while annealing at higher temperature and/or at a longer time fully destroyed the crystal quality. The optical characteristics indicate a red-shift of absorption edge in the annealed epilayers compared to the as-deposited samples, where bandgap differences were ascribed to the in-plane compressive strain relaxation during thermal annealing.²⁶ Authors ascribed that, after high temperature annealing in air and O_2 atmosphere, the nonstoichiometric GaO_x phases are reduced and the material is fully converted into Ga_2O_3 , which is accompanied by the decrease of oxygen deficiency and also the oxygen vacancy concentration.²⁶ Thus, it appears that the annealing in the temperature range of 800–900°C can induce structural and chemical changes, which in turn induce high optical transparency and bandgap values in the Ga_2O_3 films.

Conclusions

The effect of thermal annealing on the crystal structure, electronic parameters and chemical bonding in sputter-deposited nanocrystalline Ga_2O_3 films is evaluated. Increasing annealing temperature induces gradual improvement in the structural quality and packing density of the Ga_2O_3 films. Thermal annealing in air did not induce any appreciable changes in the chemical valence state of Ga ions in all of the samples. The characteristic features of Ga-O bonds that correspond to the Ga_2O_3 phase are fully evident in as-deposited and annealed samples. Raman spectroscopic measurements indicated blueshift, which may be due to confinement effect as a result of smaller crystallite size, for the high-frequency stretching and bending of the GaO_4 tetrahedra, which structurally form the $\beta\text{-}\text{Ga}_2\text{O}_3$. Spectrophotometry measurements indicate the high optical transparency of the annealed Ga_2O_3 films. The bandgap values varied in the range of 4.94–4.78 eV for a variation in annealing temperature in the range of 500–900°C. The best optical transparency and bandgap values close to that of $\beta\text{-}\text{Ga}_2\text{O}_3$ were obtained when the samples were annealed at 900°C.

Acknowledgments

The authors acknowledge, with pleasure, support from the National Science Foundation (NSF) with NSF-PREM grant #DMR-1827745. This material is also based upon work supported by the Air Force Office of Scientific Research under award number FA9550-18-1-0387. However, any opinions, finding, and conclusions or recommendations expressed in this material are those of the author(s) and do not necessarily reflect the views of the United States Air Force.

ORCID

C. V. Ramana  <https://orcid.org/0000-0002-5286-3065>

References

1. M. Higashiwaki, K. Sasaki, A. Kuramata, T. Masui, and S. Yamakoshi, *Applied Physics Letters*, **100**(1), 013504 (2012).
2. S. Roy and C. V. Ramana, *Inorganic Chemistry*, **57**, 1029 (2018).
3. L. Dong, R. Jia, B. Xin, B. Peng, and Y. Zhang, *Scientific Reports*, **7**, 40160 (2017).
4. D. Guo, H. Liu, P. Li, Z. Wu, S. Wang, C. Cui, C. Li, and W. Tang, *ACS Applied Materials & Interfaces*, **9**(2), 1619 (2017).
5. M. A. Mastro, A. Kuramata, J. Calkins, J. Kim, F. Ren, and S. Pearton, *ECS Journal of Solid State Science and Technology*, **6**(5), P356 (2017).
6. S. Pearton, J. Yang, P. H. Cary IV, F. Ren, J. Kim, M. J. Tadjer, and M. A. Mastro, *Applied Physics Reviews*, **5**(1), 011301 (2018).
7. E. J. Rubio, T. E. Mates, S. Manandhar, M. Nandasiri, V. Shutthanandan, and C. V. Ramana, *The Journal of Physical Chemistry C*, **120**(47), 26720 (2016).
8. C. V. Ramana, S. Utsunomiya, R. C. Ewing, U. Becker, V. V. Atuchin, V. S. Aliev, and V. N. Kruchinin, *Applied Physics Letters*, **92**(1), 11913 (2008).
9. Y. Yao, R. F. Davis, and L. M. Porter, *Journal of Electronic Materials*, **46**(4), 2053 (2017).
10. H. Peelaers and C. G. Van de Walle, *Physica Status Solidi (b)*, **252**(4), 828 (2015).
11. D. S. Ginley and C. Bright, *MRS Bulletin*, **25**(8), 15 (2000).
12. T. Minami, *Semiconductor Science and Technology*, **20**(4), S35 (2005).
13. M. M. Muhammed, N. Alwadai, S. Lopatin, A. Kuramata, and I. S. Roqan, *ACS Applied Materials & Interfaces*, **9**(39), 34057 (2017).
14. M. Bartic, C. I. Baban, H. Suzuki, M. Ogita, and M. Isai, *Journal of the American Ceramic Society*, **90**(9), 2879 (2007).
15. Y. Li, A. Trinchi, W. Włodarski, K. Galatsis, and K. Kalantar-zadeh, *Sensors and Actuators B: Chemical*, **93**(1–3), 431 (2003).
16. S. Ghose, S. Rahman, L. Hong, J. S. Rojas-Ramirez, H. Jin, K. Park, R. Klie, and R. Droopad, *Journal of Applied Physics*, **122**(9), 095302 (2017).
17. J. Åhman, G. Svensson, and J. Albertsson, *Acta Crystallographica Section C: Crystal Structure Communications*, **52**(6), 1336 (1996).
18. H. He, R. Orlando, M. A. Blanco, R. Pandey, E. Amzallag, I. Baraille, and M. Rérat, *Physical Review B*, **74** (19), 195123 (2006).
19. Vishal Zade, M. Bandi, S. Sanjay, A. Bronson, and C. V. Ramana, *Inorganic Chemistry*, (2019) in press.
20. G. Yang, S. Jang, F. Ren, S. J. Pearton, and J. Kim, *ACS applied materials & interfaces*, **9**(46), 40471 (2017).
21. C. V. Ramana, E. Rubio, C. Barraza, A. Miranda Gallardo, S. McPeak, S. Kotru, and J. Grant, *Journal of Applied Physics*, **115**(4), 043508 (2014).
22. R. Rao and A. M. Rao, *Journal of Applied Physics*, **98**, 094312 (2005).
23. D. Dohy, G. Lucaleau, and A. Revcoleschi, *J. Solid State Chem.*, **45**, 180 (1982).
24. M. Rebien, W. Hong Henrion, J. P. Mannaerts, and M. Fleischer, *Applied Physics Letters*, **81**, 250 (2002).
25. Qiong Cao, Linan He, Xianjin Feng, Hongdi Xiao, and Jin Ma, *Ceramics International*, **44**, 830 (2018).
26. Z. Feng, L. Huang, G. Feng, X. Li, H. Zhang, W. Tang, J. Zhang, and Y. Hao, *Optical Materials Express*, **8**, 2229 (2018).